Effect of substituting Fe by Mn in GdFeO$_3$ perovskite catalyst for CO hydrogenation

A. A. Sharaeva[1*], T. F. Sheshko[1], T. A. Kryuchkova[1], L. V. Yafarova[2], I. A. Zvereva[2]

[1]*Peoples' Friendship University of Russia (RUDN University), Faculty of Science, Physical and Colloidal Chemistry Department, Miklukho-Maklaya str. 6, Moscow, 117198 Russia*
[2]*Saint-Petersburg State University, Petrodvorets, Universitetsky pr. 26, Saint-Petersburg, 198504 Russia*

Gd(Fe,Mn)O$_3$ nanoperovskites were prepared by sol-gel method and were characterized using different techniques: XRD, SEM+EDX, BET, TG to study structure and morphology. Oxidation states of Fe and Mn were determined by XPS. The performance of GdFe$_{1-x}$Mn$_x$O$_3$ perovskite catalysts with different Mn substitution levels was evaluated in the CO hydrogenation for light olefins production. The complex of physico-chemical methods showed that all investigated samples confirmed the presence of a single phase with perovskite-type structure. Experimental data suggested that catalysts can operate over a wide temperature range without any loss of activity and are practically unaffected by surface carbonation; their phase composition and morphology of the surface change insignificantly in catalytic processes at high temperature (~ 673 K). It was determined that the introduction of manganese into perovskite structure led to a change in the quantitative composition: the amount of butylene was much higher than that of ethylene on the samples containing manganese in the B-site. Activation of catalytic centers and their further stabilization taking place under the action of the reaction medium was established for all the systems studied.

Keywords: carbon monoxide hydrogenation, perovskite catalysts, light olefins, Fischer-Tropsch synthesis

INTRODUCTION

Fischer-Tropsch synthesis (carbon monoxide hydrogenation) converts syngas (mixture of carbon monoxide and hydrogen) into hydrocarbons and oxygenates. The syngas for CO hydrogenation can be produced from fossils and renewable resources (natural gas, coal, carbon residues, and biomass), making this reaction suitable for manufacturing alternative sustainable liquid fuels.

Different types of catalysts with a wide range of metal atoms have been studied, such as higher alcohol synthesis catalysts (based on Cu, Zn, Cr, Al) [1-3], modified Fischer-Tropsch synthesis catalysts (based on Fe, Co, Mn) [4-7] and molybdenum-based catalysts [8]. Zhao *et al.* [9] reported about technologies like MTO (methanol to olefins) and SDTO (synthesis gas through dimethyl ether to olefins) that are already used in industry on zeolite catalysts. However, high operating costs and rapid deactivation of the catalyst, as well as low selectivity to $C_2^=$- $C_4^=$ hydrocarbons are the main disadvantages of these technologies in industrial applications.

Recently, perovskite oxides with an ABO$_3$ type structure (where A and B represent different metallic elements) have been studied for light olefins production [10].

Partial substitution at the A- or/and B-sites of the perovskite (ABO$_3$) leads to changes in the perovskite structure, the oxygen mobility and the redox properties of the perovskite, which affects the catalytic activity. Partial substitution at the B-site was found to be an effective method for improvement of product selectivity in carbon monoxide hydrogenation. In our previous work [11], we have reported about catalytic properties of GdFe$_{1-x}$Mn$_x$O$_3$ (x = 0, 0.01, 0.05, 0.2, 0.5, 0.8 and 1) nanoperovskites prepared by ceramic and sol-gel method. The highest stability, catalytic activity, and unsaturated hydrocarbons (ethylene and propylene) selectivity in the carbon oxides hydrogenation were achieved over GdFeO$_3$, GdFe$_{0.95}$Mn$_{0.05}$O$_3$, 5 %wt Mn/GdFeO$_3$ samples.

The main objective of this study is to investigate the effect of manganese substitution on the catalytic activity of GdFeO$_3$ perovskite in syngas conversion, and to find correlation between the composition of complex oxides and their catalytic activity.

EXPERIMENTAL

Catalyst preparation

A series of GdFe$_{1-x}$Mn$_x$O$_3$ (x=0, 0.5, 0.8 and 1) perovskite-type oxides were synthesized *via* sol–gel method in which citric acid (C$_6$H$_8$O$_7$·H$_2$O) was used as the complexing agent. Gd(NO$_3$)$_3$·5H$_2$O, Fe(NO$_3$)$_3$·9H$_2$O and Mn(NO$_3$)$_2$·4H$_2$O were mixed and dissolved in deionized water. The solution was heated and vigorously stirred until the temperature reached 363-373K, citric acid was added to the

---

solution at that moment. Ammonia solution was used to maintain pH = 6. Thereafter, it was slowly heated up to ~393K until self-ignition of the gel obtained and formation of black powder occurred. The resulting powder was calcined *via* increasing the temperature from ambient one to 723K and the maximum temperature remained constant for 2 h in order to obtain perovskite phases with the same order of crystallinity.

Catalyst characterization

X-ray diffraction data were determined at room temperature on ARL X'TRA and Rigaku "MiniFlex II" devices using CuKα radiation. The surface morphology and microstructure of the samples was investigated by scanning electron microscopy (SEM) by Zeiss EVO®40 microscope and a Carl Zeiss Supra 40VP electron microscope. Specific surface area measurements were carried out by using Brunauer-Emmett-Teller (BET) method based on N_2 adsorption at 77 K on Nova 4200e instrument (Quantachrome). X-ray photoelectron spectroscopy (XPS) of the samples was performed using a Thermo Fisher Scientific Escalab 250Xi with Al Kα (λ = 0.1541 nm) radiation which was used for material excitation.

Catalytic activity measurements

The catalyst performance in CO hydrogenation was evaluated in a fixed-bed quartz U-shaped tubular reactor, containing ~0.1 g of sample. The samples were diluted using quartz particles with a mesh size of 0.25-0.5 mm. The reactor was imbedded in an insulated electric furnace, equipped with a temperature programmable controller. The experiments were carried out in the temperature range from 523 to 708K under atmospheric pressure with a feed composition of $CO:H_2 = 1:2$ and a total flow of 1.5 L/h, with a continuous feed of the reactants. The reactor was placed vertically in the center of a tubular furnace and its temperature was measured/controlled by a K-type thermocouple, placed in the center of the catalyst bed without direct contact with the catalyst.

The temperature was increased from 523 to 708K and remained steady for the desired reaction time. All catalytic reactions were conducted at this temperature. Each experiment took about 7 h. In all experiments the perovskite catalyst was used without previous reduction. The streams were analyzed with a gas chromatograph (Crystal 5000.2, Russia) equipped with thermal conductivity and flame ionization detectors, stainless steel column packed with Porapack Q for detecting reaction products. The rate of formation the reaction products R or space time yields (STY) (mol/h*g_{cat}) was measured after the system reached

an equilibrium state, estimated from the constant chromatographic peaks and normalized per unit mass of catalyst.

The rate of formation of the reaction products R (mol/h*g_{cat}) and the product selectivity (S_i) were calculated according to the following equations:

CO conversion (X_{CO}, % by moles)

$$X_{CO}(\%) = \frac{\text{Moles CO}_{in} - \text{Moles CO}_{out}}{\text{Moles CO}_{in}} \times 100\% \qquad (1)$$

The rate of formation of the reaction products R (mol/h*g_{cat}) was calculated as:

$$R_i = \frac{K_X S_i w}{V_{loop} m_{cat.}} \qquad (2)$$

where, K_x – correction factor for the i-reaction product; S_i – chromatographic peak area, mV/min; R_i – the rate of formation of the i-reaction product per 1 g of catalyst, mol/h*g_{cat}; w – reaction space velocity, 1 – 1.5 L/h; V_{loop} – chromatography sample loop volume, 0.001 L; $m_{cat.}$ – the mass of the catalyst metal phase, g.

C_n selectivity (% by C-atoms):

$$S_i = \frac{R_i}{\sum R_i} \times 100\% \qquad (3)$$

where, R_i – the rate of formation of the i-reaction product per 1 g of catalyst, mol/h*g_{cat}; $\sum R_i$ – the sum of the rates of formation of the i-reaction products per 1 g of catalyst, mol/h*g_{cat}.

RESULTS AND DISCUSSION

Catalyst characterization

In the literature the complex oxide GdFeO₃ [12] is described as an oxide with a distorted perovskite structure. The results in Fig 1 show the X-ray phase analysis of samples of GdFeO₃, GdMnO₃ and GdMn₀.₅Fe₀.₅O₃. All diffractograms are typical for compounds with a well-pronounced perovskite crystal structure. Peaks refer to single-phase GdFeO₃, GdMnO₃ and GdMn₀.₅Fe₀.₅O₃ (PDF cards 01-072-9906, 01-070-9199) these connections have an orthorhombic structure. The diffractogram of the synthesized GdMn₀.₅Fe₀.₅O₃ is similar with that described in the reported research [13]

Representatives of scanning electron microscopy images of GdFeO₃, GdMnO₃ and GdMn₀.₅Fe₀.₅O₃ samples are shown in Fig. 2. SEM images of GdMnO₃ and GdMn₀.₅Fe₀.₅O₃ samples show a porous structure with uniformly distributed size grains ~ 200 nm before the catalytic process. The morphology of GdFeO₃ particles is somewhat different from that of particles with paramagnetic Fe and Mn ions: polycrystals are more elongated with an average diameter of 30–60 nm and a length of about 200 nm.
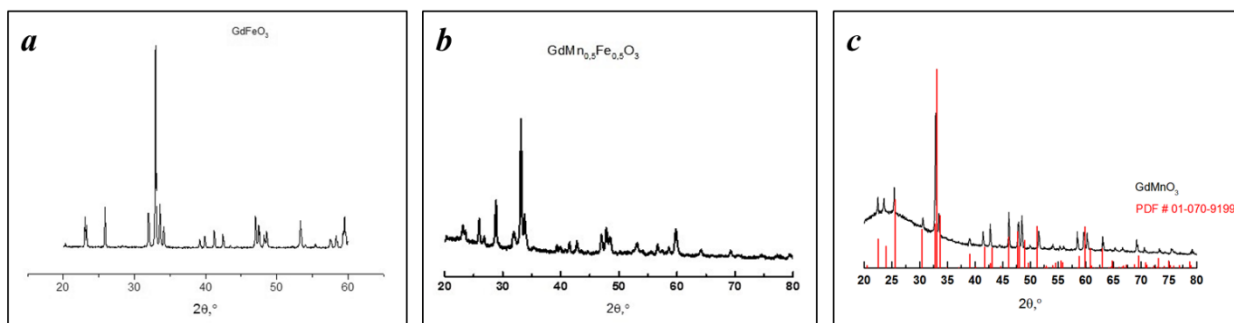
Figure 1. XDR patterns of complex oxides: *(a)* $GdFeO_3$; *(b)* $GdMnO_3$; *(c)* $GdMn_{0.5}Fe_{0.5}O_3$
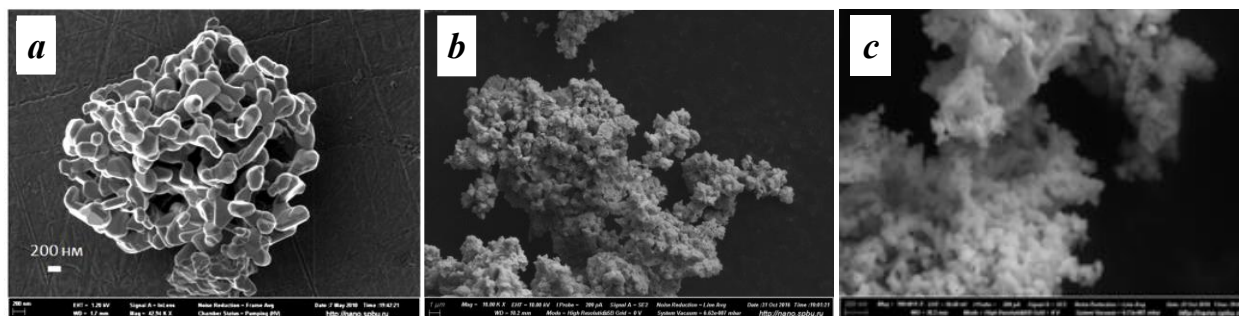
Figure 2. SEM images of $GdFe_{1-x}Mn_xO_3$ complex oxide: *(a)* x=0, *(b)* x=0.5, *(c)* x=1
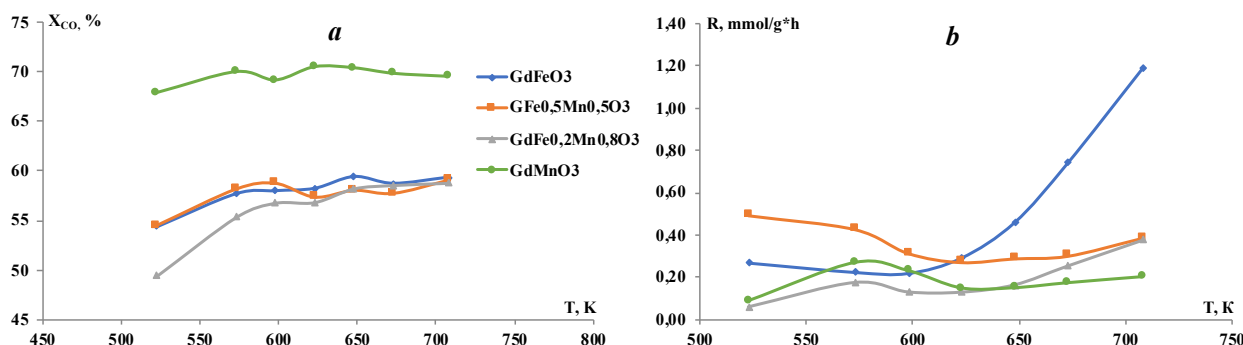
Figure 3. Temperature dependence of (a) the CO conversion and (b) the rate of formation of CO_2 (at a ratio of $CO:H_2 = 1:2$)

Mössbauer spectra of the solid solutions synthesized *via* sol–gel technology showed the iron atoms in the $GdFeO_3$ samples to be in state Fe^{3+} in two fields with different symmetry.

The XPS spectra of $GdFe_{1-x}Mn_xO_3$ and $GdMnO_3$ samples have the satellite peak at 641.8 eV present in the spectra, which corresponds to the state of Mn^{3+}. [14] The Fe2p spectrum showed that iron is in the Fe^{3+}[15] state. Gd^{3+} in all compounds before and after catalysis did not change the degree of oxidation.

Catalytic data

Carbon monoxide hydrogenation was carried out within the temperature range of 523-708 K, with a ratio of $CO: H_2 = 1: 2$. The conversion of CO on all samples is given in Fig. 3a: it was 50–70% and varied slightly with increasing temperature, and on $GdMnO_3$ it turned out to be a little higher. The formation of CO_2 in the catalytic temperature range

was observed (Fig. 3b), the CO_2 amount on all studied $GdFe_{1-x}Mn_xO_3$ perovskites, in the temperature range 596-708 remained approximately the same.

Since the course of the curves describing the temperature dependences of CO conversion and CO_2 content in the reaction mixture on the studied catalysts did not differ significantly, it can be assumed that only carbon particles are involved in the formation of reaction products resulting from dissociative adsorption in the noncatalytic temperature range. The CO_2 formation becomes possible when the adsorbed CO_{ads} molecule interacts either with perovskite surface oxygen (O_S) or with oxygen released during dissociative adsorption of CO [16]: $CO_{ads} + O_S \rightarrow CO_2$

Since catalytic synthesis proceeds through the interaction of chemisorbed reagents, it is logical to expect a correlation of the catalytic activity and

transition metals selectivity with both absolute heat values of CO and H_2 adsorption on the surface of metals, and with their difference, in the first approximation. According to [17], the difference in the energy of adsorption of CO and H_2 on the surface decreases in the series of Mn, Fe, Co, and these energies themselves are not too large, and therefore the energy barrier to the reaction of adsorbed CO and H_2 will be small. Furthermore. the energy of the bond Me - CO increases in the same series of Mn, Fe, Co. These results [17] correlate well with the obtained CO conversions values.

The reaction products were C_1-C_6 hydrocarbons over all catalytic systems. Among them there are the main ones: methane, ethylene, propylene, butylene. The product formation started at 523K, and further increased with the temperature, but at T> 623 K the rate of C_3-C_6 hydrocarbons formation went down. For example, Fig. 4 shows the temperature dependences of the hydrocarbons formation rates during the reaction conducted on GdMnO₃. The results from Table 1 clearly demonstrate that increasing the amount of manganese in the B-site of the perovskite structure leads to decline of the products formation rate in the following order: GdFeO₃ > GdFe₀.₅Mn₀.₅O₃ > GdFe₀.₂Mn₀.₈O₃ > GdMnO₃.

Varying the composition of the catalysts caused changes in the reaction products ratio that can be seen in Table 2. So, in the case of using GdFeO₃ as a catalyst, the amount of methane and light olefins in the reaction mixture at T = 673 K was 71% and 26%, respectively and over complex oxides with partial or full substitution of iron by manganese, the methane content decreased to 30%, and olefins increased to 35%, as well as the hydrocarbons C_5-C_6 ratio.
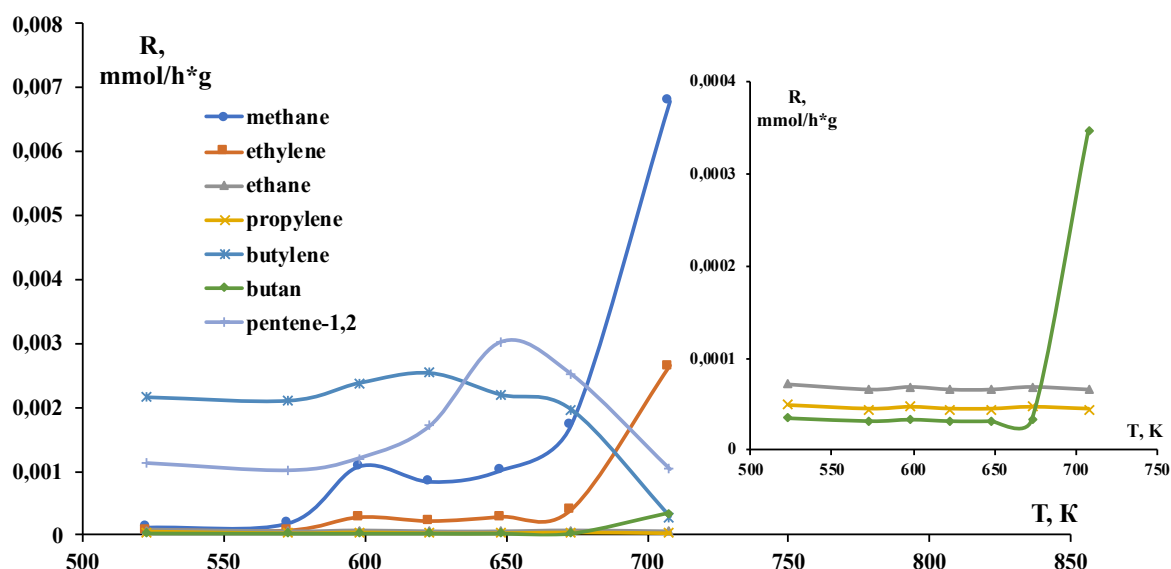
Figure 4. The temperature dependences of the hydrocarbons formation rates over GdMnO₃ (at ratio of CO:H_2=1:2)

Table 1. The rates of formation C_1, $C_2^=$, $C_4^=$, CO_2 (at T = 708 K)

Sample	R(CH₄), mcmol/h*g_cat	R(C₂H₄), mcmol/h*g_cat	R(C₄H₈), mcmol/h*g_cat	R(CO₂), mcmol/h*g_cat
GdFeO₃	2536.0	727.0	0.3	1190.0
GdFe₀.₅Mn₀.₅O₃	99.3	22.9	1.0	387.0
GdFe₀.₂Mn₀.₈O₃	17.0	6.2	0.7	375.0
GdMnO₃	66.8	2.6	0.3	201.0

Table 2. Products composition of carbon monoxide hydrogenation process (at T = 673 K)

Sample	S(CH₄), %	S(C₂H₄), %	S(C₃H₆), %	S(C₄H₈), %	S(C₅-C₆), %
GdFeO₃	71.07	18.37	7.29	0.08	3.19
GdFe₀.₅Mn₀.₅O₃	61.26	17.00	7.97	7.37	6.39
GdFe₀.₂Mn₀.₈O₃	27.53	6.31	2.99	28.10	35.06
GdMnO₃	25.01	5.65	0.68	28.61	40.05
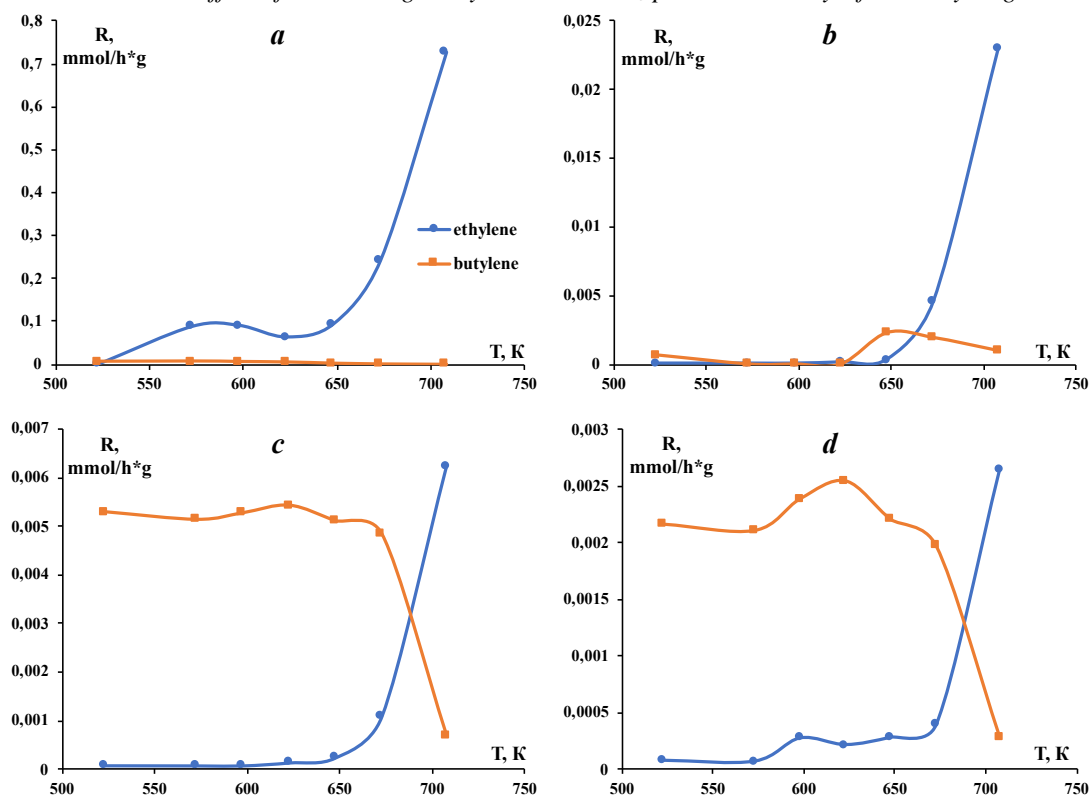
Figure 5. The temperature dependences of ethylene and butylene production rates over $GdFe_{1-x}Mn_xO_3$ perovskite catalysts: *(a)* x=0, *(b)* x=0.5, *(c)* x=0.8, *(d)* x=1

Table 3. Experimental values of activation energy and pre-exponential factor

Catalyst	$E_a(CH_4)$, kJ/mol	$Ln\ K_0(CH_4)$	$E_a(C_2H_4)$, kJ/mol	$Ln\ K_0(C_2H_4)$
$GdFeO_3$	70	5.70	65	3.49
$GdFe_{0.5}Mn_{0.5}O_3$	135	15.81	131	13.21
$GdFe_{0.2}Mn_{0.8}O_3$	87	4.76	102	6.79
$GdMnO_3$	67	-1.05	98	3.46

It should be noted that carrying out the reaction over GdFeO₃, ethylene prevailed in products among olefins and butylene was practically absent while on samples with manganese in the anionic sublattice of perovskite at low temperatures butylene prevailed (Fig. 5). An increase in temperature resulted in lower rates of butylene formation and sharp increase in ethylene production rates.

For assessing the activation energy and the number of active centers on the surface test data were processed in linear references of the Arrhenius equation.

The results in Table 3 show that an increase in the manganese fraction in the samples, with the exception of GdFe₀.₅Mn₀.₅O₃, led to a decrease in the pre-exponential factor logarithms, in this case, the activating energies did not change significantly. It was suggested that the decrease in the number of active centers affected the decrease in the rates of formation of products. The higher values of

activation energies for the sample with the stoichiometric content of iron and manganese were observed with a sufficiently large number of active centers. The reason why fall in speeds may be due to the "competition" between active centers can be assumed.

In [18] it was found that the introduction of manganese oxide into the supported iron-containing catalyst leads to a significant increase in the selectivity to olefins in the co-hydrogenation of carbon oxides. It was suggested that the iron-generated CHₓ radicals are transported through the gas phase ("jumper effect") onto the surface of manganese oxide, on which sorbed hydrogen is practically absent, where they are subsequently recombined into olefins. The differences in the catalytic activity of the samples are due to the different diffusion rates of weakly bound atomic hydrogen (H_I) over the surface of the catalysts (spillover effect). The results obtained by us are in good agreement with this assumption: at low

temperatures, on samples containing manganese, the CH_x-radicals interact with each other, leading to the formation of mainly butylene. An increase in the temperature of the process leads to an increase in the mobility of both CH_x particles and atomic hydrogen, which leads to an increase in the amount of ethylene produced. The calculation of the total selectivities for olefins showed that the introduction of manganese in the B-position of the perovskite lattice leads to an increase in the selectivity of the process with respect to light olefins C_2-C_4 (Fig. 6). So, if on ferrite selectivity was 25% -30%, then for samples where manganese prevailed, it reached 80%.

All the tested catalysts showed a high stability. It was established that the phase composition of all ferrites remains unchanged after catalytic reactions. Partial decomposition of catalysts and significant changes in the samples morphology did no occur. Catalytic characteristics were preserved during the repeated experiments and were not changed after 50 hours of the experiment. The mass change of the catalyst after completion of all tests did not exceed 1% for all investigated systems. It may indicate a slight carbonization surface of the tested ferrites and their potential use in further studies.
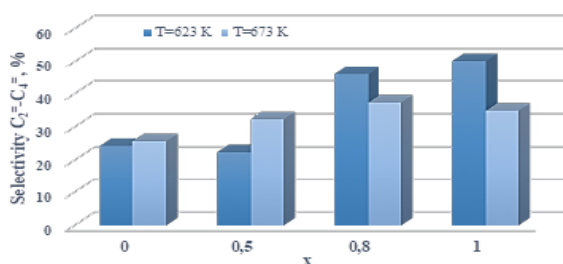
Figure 6. Correlation between CO selectivity and composition of the catalysts.

CONCLUSIONS

$GdFe_{1-x}Mn_xO_3$ perovskite catalysts were successfully synthesized by sol-gel method. The effect of different additions the Mn on the catalytic performance and the quantitative ratio of the products of hydrogenation was investigated. The $x(Mn) = 1$ perovskite displays a content of methane and light olefins of 71% and 26%, respectively, at T = 673 K. While on complex oxides with partial or full substitution of Fe by Mn ($x(Mn) = 0.5, 0.8, 1$) the amount of methane decreased to 40%, and olefins increased to 35%, while increasing the proportion of hydrocarbons C_5-C_6. It was found that $GdMnO_3$ catalyst has shown better selectivity for light olefins (ethylene and butylene) production while the highest catalytic activity in the carbon oxides hydrogenation was obtained over $GdFeO_3$.

REFERENCES

1. S. M. Choi, Y. J. Kang, S. W. Kim, *Applied Catalysis A, General*, **549**, 188 (2018).
2. T.-W. Kim, F. Kleitz, J. Won Jun, H.-J. Chae, Ch.-U. Kim, *Journal of Industrial and Engineering Chemistry* **51**, 196 (2017).
3. E. Heracleous, E. T. Liakakou, A. A. Lappas, A. A. Lemonidou, *Applied Catalysis A: General,* **455**, 145 (2013).
4. E. van Steen, M. Claeys, K.P. Möller, D. Nabaho, *Applied Catalysis A, General,* **549**, 51 (2018).
5. J.-L. Zhang, X. Wang, L.-P. Ma, X.-F. Yu, Q.-X. Ma, S.-B. Fan, T.-S. Zhao, *J. Fuel Chem. Technol.*, 45, 1489 (2017).
6. J.-L. Zhang, L.-H. Ma, S.-B. Fan, T.-Sh. Zhao, Y.-H. Sun, *Fuel*, **109** 116 (2013).
7. M. Arsalanfar, A. A. Mirzaei, H. R. Bozorgzadeh, A. Samimi, R. Ghobadi, *Journal of Industrial and Engineering Chemistry*, **20**, 1313 (2014).
8. T. Li, M. Virginie, A. Y. Khodakov, *Applied Catalysts A, General,* **542**, 154 (2017).
9. M. Zhao, Y. Cui, J. Sun, Q. Zhang, *Catalysis Today*, **316**, 142 (2018).
10. N. Escalona, S. Fuentealba, G. Pecchi, *Applied Catalysis A: General*, **381**, 253 (2010).
11. T. Sheshko, T. Kryuchkova, Yu. Serov, A. Shulga, I. Chislova, L. Yafarova, I. Zvereva, NANOCON 2017, Brno, Czech Republic, EU 187-192.
12. B.S. Mathur, H. Shen, N. Lecerf, A. Kjekshus, H. Fjellvaag, G. F. Goya, *Adv. Mater. (Weinheim, Ger.)* **14** 19, 1405 (2002); Inst. Anorg. Chem., Univ. des Saarlandes, D-66123 Saarbruecken, Germany; Eng.
13. M. Romero, R. Faccio, J. Martinez, H. Pardo, B. Montenegro, C. Campos Pla Cid, A. A. Pasa, A. W. Mombru, *Journal of Solid State Chemistry*, **221**, 325 (2015).
14. J. F. Moulder, W. F. Stickle, P. E. Sobol, K. D. Bomben, Handbook of X-ray photoelectron spectroscopy: a reference book of standard spectra for identification and interpretation of XPS data, Surf. Interface Anal., 1992, p. 261.
15. H. Liu, G. Wei, Z. Xu, P. Liu, Y. Li, *Appl. Surf. Sci.*, **389**, 438 (2016).
16. A. L. Lapidus, A. Yu. Krylova, *Russian Journal of General Chemistry*, **44**, 43 (2000).
17. P. C. Keith, *Oil Gas J.*, **45**, 102 (1946).
18. T. F. Sheshko, Yu. M. Serov, *Russ. J. Phys. Chem. A.* **86**, 283 (2012).